



**HAL**  
open science

# Safety and Efficacy of Avaren-Fc Lectibody Targeting HCV High-Mannose Glycans in a Human Liver Chimeric Mouse Model

Matthew Dent, Krystal Hamorsky, Thibaut Vausselin, Jean Dubuisson,  
Yoshinari Miyata, Yoshio Morikawa, Nobuyuki Matoba

► **To cite this version:**

Matthew Dent, Krystal Hamorsky, Thibaut Vausselin, Jean Dubuisson, Yoshinari Miyata, et al.. Safety and Efficacy of Avaren-Fc Lectibody Targeting HCV High-Mannose Glycans in a Human Liver Chimeric Mouse Model. Cellular and Molecular Gastroenterology and Hepatology, 2020, 10.1016/j.jcmgh.2020.08.009 . hal-02992405

**HAL Id: hal-02992405**

**<https://hal.science/hal-02992405>**

Submitted on 6 Nov 2020

**HAL** is a multi-disciplinary open access archive for the deposit and dissemination of scientific research documents, whether they are published or not. The documents may come from teaching and research institutions in France or abroad, or from public or private research centers.

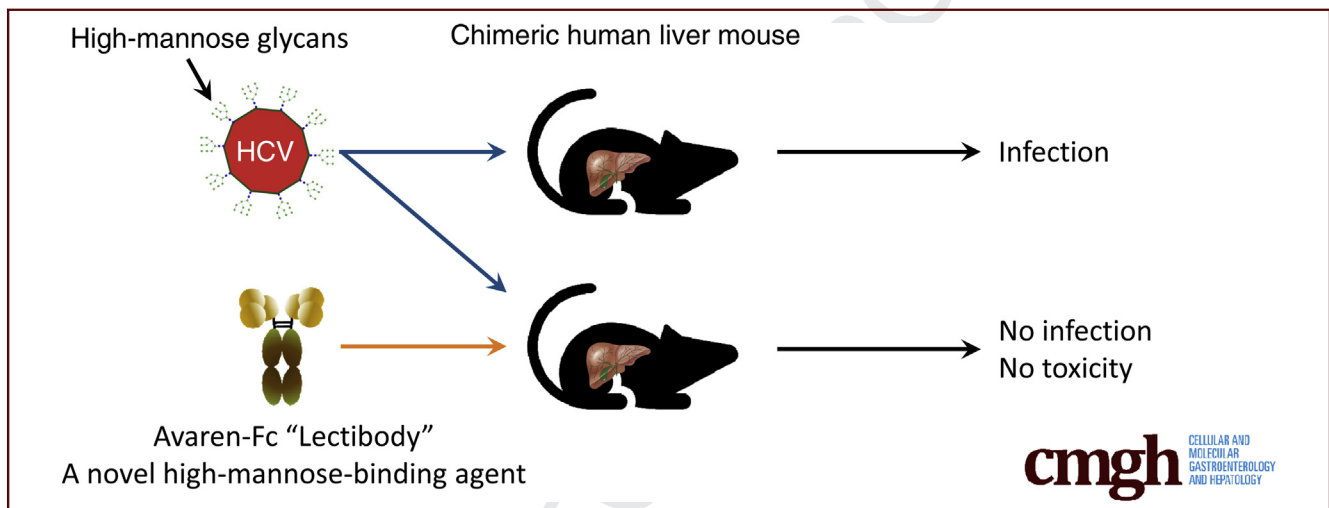
L'archive ouverte pluridisciplinaire **HAL**, est destinée au dépôt et à la diffusion de documents scientifiques de niveau recherche, publiés ou non, émanant des établissements d'enseignement et de recherche français ou étrangers, des laboratoires publics ou privés.

## ORIGINAL RESEARCH

## Safety and Efficacy of Avaren-Fc Lectibody Targeting HCV High-Mannose Glycans in a Human Liver Chimeric Mouse Model

Matthew Dent,<sup>1</sup> Krystal Hamorsky,<sup>2,3,4</sup> Thibaut Vausselin,<sup>5</sup> Jean Dubuisson,<sup>5</sup>  
Yoshinari Miyata,<sup>6</sup> Yoshio Morikawa,<sup>6</sup> and Nobuyuki Matoba<sup>1,3,4</sup>

<sup>1</sup>Department of Pharmacology and Toxicology, <sup>2</sup>Department of Medicine, <sup>3</sup>James Graham Brown Cancer Center, <sup>4</sup>Center for Predictive Medicine, University of Louisville School of Medicine, Louisville, Kentucky; <sup>5</sup>University of Lille, CNRS, INSERM, CHU Lille, Institut Pasteur de Lille, U1019, UMR 8204, Center for Infection and Immunity of Lille, Lille, France; <sup>6</sup>PhoenixBio USA Corporation, New York, New York



## SUMMARY

Hepatitis C virus (HCV) infection remains a major cause of end-stage liver disease. Here, we show the efficacy and safety of a novel biotherapeutic targeting a HCV glyco-biomarker in a mouse model, providing a foundation for a new anti-HCV strategy.

**BACKGROUND & AIMS:** Infection with hepatitis C virus (HCV) remains a major cause of morbidity and mortality worldwide despite the recent advent of highly effective direct-acting antivirals. The envelope glycoproteins of HCV are heavily glycosylated with a high proportion of high-mannose glycans (HMGs), which serve as a shield against neutralizing antibodies and assist in the interaction with cell-entry receptors. However, there is no approved therapeutic targeting this potentially druggable biomarker.

50% inhibitory concentration values in the low nanomolar range. Systemic administration of AvFc in a histidine-based buffer was well tolerated; after 11 doses every other day at 25 mg/kg there were no significant changes in body or liver weights or in blood human albumin or serum alanine aminotransferase activity. Gross necropsy and liver pathology confirmed the lack of toxicity. This regimen successfully prevented genotype 1a HCV infection in all animals, although an AvFc mutant lacking HMG binding activity failed.

**CONCLUSIONS:** These results suggest that targeting envelope HMGs is a promising therapeutic approach against HCV infection, and AvFc may provide a safe and efficacious means to prevent recurrent infection upon liver transplantation in HCV-related end-stage liver disease patients. (*Cell Mol Gastroenterol Hepatol* 2020; ■:■-■; <https://doi.org/10.1016/j.jcmgh.2020.08.009>)

**Keywords:** Hepatitis C Virus; Entry Inhibitor; Plant-Made Pharmaceutical; High-Mannose Glycan; Antiviral Therapy.

Hepatitis C virus (HCV) is an enveloped monopartite positive-sense single-strand RNA virus in the family *Flaviviridae* and the causative agent of hepatitis C disease. Its genome encodes 3 structural (core, E1, E2) and 7 nonstructural proteins (p7, NS2, NS3, NS4A, NS4B, NS5A,

and NS5B).<sup>1</sup> HCV is highly heterogenous and distributed globally, consisting of 7 genotypes, each subdivided further into multiple subtypes. Genotypes 1 and 2 are the predominant genotypes worldwide and are particularly concentrated in high-income and upper-middle-income countries, whereas genotypes 3 and 4 are more common in lower-middle and low-income countries.<sup>2</sup> In the United States, injection drug use represents the primary risk factor for contracting HCV infection.<sup>3,4</sup> Approximately 15%–25% of people acutely infected with HCV will clear the virus, while the remainder will develop chronic infection that can persist largely unnoticed for decades. Indeed, many HCV carriers discover their chronic infection after they have developed cirrhosis.<sup>5</sup> Chronic HCV infection also is associated with the development of hepatocellular carcinoma, and patients with the disease are more likely to develop cryoglobulinemia and non-Hodgkin's lymphoma.<sup>6</sup>

There is no vaccine currently available for HCV. Before 2011, the standard chronic HCV treatment was a nonspecific antiviral medication using ribavirin combined with pegylated interferon- $\alpha$ , which was associated with significant toxicity and limited treatment efficacy.<sup>7</sup> In 2011, the US Food and Drug Administration approved the first-generation of direct-acting antivirals (DAAs) for HCV: boceprevir and telaprevir, both of which inhibit the viral protease (NS3/4A), but required co-treatment with ribavirin and peginterferon.<sup>8,9</sup> Further approval of more potent DAAs, such as NS3/4A, NS5B, and NS5A inhibitors, led to the development of oral ribavirin/peginterferon-free regimens.<sup>5</sup> Multi-DAA regimens achieve sustained virologic response (defined as a period of time with no viral RNA detection) rates as high as 100%, and are less toxic and more tolerable than their predecessors.<sup>10–13</sup> Although the cure rates are remarkable, populations of patients exist who may not benefit from DAA therapy,<sup>14</sup> especially patients with decompensated cirrhosis resulting from chronic HCV infection, for whom liver transplantation may be a last resort.<sup>15</sup> Moreover, recurrent infection occurs universally and rapidly after liver transplantation,<sup>16,17</sup> which increases the risk of accelerated cirrhosis, graft failure, and death.<sup>18</sup> DAAs, by their nature, cannot prevent recurrent infection. Therefore, alternative or complementary therapies to DAAs that can block viral entry to target cells, such as antibodies or other molecules acting alike, may need to be considered in these circumstances.<sup>18,19</sup> However, there is currently no entry inhibitor approved for HCV treatment.

The HCV envelope proteins E1 and E2 are heavily glycosylated and, similar to glycoproteins of other enveloped viruses (eg, human immunodeficiency virus [HIV] and the coronaviruses), have a high proportion of high-mannose-type *N*-glycans (HMGs) on their surface.<sup>20–22</sup> These glycans typically are processed to hybrid and complex forms on glycoproteins secreted by healthy cells.<sup>23</sup> Thus, the HMGs on the surface of HCV may be considered a druggable target. We previously described the development of an HMG-targeting lectin-Fc fusion protein, or *lectibody*, called Avaren-Fc (AvFc), which was shown to bind with high affinity to clusters of HMGs on the HIV envelope protein glycoprotein (gp)120 and effectively neutralize multiple HIV

clades and groups including HIV-2 and simian immunodeficiency virus.<sup>24</sup> Further analysis indicated that AvFc can bind to HCV E2 protein.<sup>24</sup> Therefore, in this study, we aim to investigate the anti-HCV therapeutic potential of AvFc in *in vitro* neutralization assays and an *in vivo* HCV challenge study using PXB mice, a chimeric urokinase plasminogen activator/severe combined immunodeficiency (uPA/SCID) mouse model transplanted with human hepatocytes (reviewed by Tateno and Kojima<sup>25</sup>).

## Results

### AvFc Shows Broad Anti-HCV Activity *In Vitro*

Building on our previous observation that AvFc has affinity to a recombinant HCV E2 envelope protein,<sup>24</sup> we first examined whether AvFc inhibits HCV infection *in vitro* using multiple genotypes of cell culture-produced virus (HCVcc) or pseudotyped virus (HCVpp). AvFc significantly blocked the infection of the human liver cell line Huh-7 by HCVcc from genotypes 1a, 2a, 4a, 5a, and 6a, with 50% inhibitory concentration values in the low nanomolar range (Table 1 and Figure 1A). Compared with Avaren monomer, AvFc overall showed approximately 2-log higher activity, although no inhibitory effect was observed for the plant-produced anti-HIV broadly neutralizing antibody VRC01, which shares the same human IgG1 Fc region with AvFc.<sup>26</sup> In addition, Avaren and AvFc, but not VRC01, effectively neutralized HCVpp harboring a murine leukemia virus backbone, suggesting that the lectin and the lectibody act as an entry inhibitor (Figure 1B).

### Formulation of AvFc Into a Biocompatible Buffer for *In Vivo* Studies

Previously, we found that AvFc has limited solubility in phosphate-buffered saline (PBS) at concentrations greater than 1 mg/mL (unpublished observation). To facilitate *in vivo* studies, we screened for an optimal liquid formulation for systemic administration that can impart improved stability and solubility to AvFc at higher concentrations. Initial buffer screening showed that AvFc is prone to degradation at and below a pH of 6.5, suggesting that AvFc is not stable in acidic pH conditions (Figure 2, Table 2). Further preformulation studies led us to identify an optimal buffer composed of 30 mmol/L histidine, pH 7.0, 100 mmol/L sucrose, and 100 mmol/L NaCl. Although AvFc showed comparable melting temperature in the histidine buffer and PBS in differential scanning fluorimetry ( $62.49^{\circ}\text{C} \pm 0.13^{\circ}\text{C}$

**Abbreviations used in this paper:** ALT, alanine aminotransferase; AvFc, Avaren-Fc; DAA, direct-acting antiviral; h-Alb, human albumin; HCV, hepatitis C virus; HCVcc, cell-culture-derived hepatitis C virus; HCVpp, hepatitis C virus pseudovirus; HIV, human immunodeficiency virus; HMG, high-mannose glycans; JFH, \_\_\_\_\_; PBS, phosphate-buffered saline; RT-PCR, reverse-transcription polymerase chain reaction; uPA/SCID, urokinase plasminogen activator/severe combined immunodeficiency.

© 2020 The Authors. Published by Elsevier Inc. on behalf of the AGA Institute. This is an open access article under the CC BY license (<http://creativecommons.org/licenses/by/4.0/>).

2352-345X

<https://doi.org/10.1016/j.jcmgh.2020.08.009>

**Table 1.** IC<sub>50</sub> Values for AvFc and Avaren Against HCVcc

Virus	Genotype	Avaren IC <sub>50</sub> , nmol/L	AvFc IC <sub>50</sub> , nmol/L
JFH1/H77	1a	529.28 ± 158.78	1.69 ± 0.39
JFH1	2a	484.62 ± 109.16	1.69 ± 0.78
JFH1/ED43	4a	204.27 ± 1.65	2.85 ± 0.91
JFH1/SA13	5a	148.86 ± 2.48	2.33 ± 0.13
JFH1/HK6a	6a	114.95 ± 52.93	1.95 ± 0.78
	Average	269.39 ± 65.00	2.10 ± 0.60

IC<sub>50</sub>, 50% inhibitory concentration.

vs 62.68°C ± 0.25°C) (Figure 3A), sodium dodecyl sulfate–polyacrylamide gel electrophoresis analysis showed that the lectin body holds superior stability in the histidine buffer upon accelerated stability testing via overnight incubation at 55°C (Figure 3B). When concentrated to approximately 10 mg/mL, AvFc remained stable in solution in the histidine buffer over 72 hours at 4°C and room temperature, while showed a significant concentration decrease concomitant with increasing turbidity in PBS (Figure 3C), further showing the histidine buffer's superiority for AvFc formulation.

### Pharmacologic and Toxicologic Analysis of AvFc in Mice

To determine an optimal dosing regimen for an HCV challenge experiment, a pharmacokinetic analysis of AvFc was conducted in C57bl/6 mice. After a single

intraperitoneal injection of AvFc at a dose of 25 mg/kg, a peak drug concentration was observed between 2 and 4 hours, with a half-life of 24.5 hours in male animals and 18.5 hours in female animals (Figure 4). After 48 hours, in both male and female animals, the plasma concentration of AvFc remained above a target trough concentration of 130 nmol/L (10 µg/mL), at which time AvFc showed more than 90% neutralization effects against HCV (Figure 1). Consequently, these results suggested that administration of the drug every other day might be sufficient to keep the virus under control in a murine HCV challenge model.

We then assessed the safety of every-other-day administration of AvFc in PXB mice. To effectively discern potential toxicity associated with AvFc HMG-binding activity, we included an AvFc variant lacking HMG-binding activity as a control (AvFc<sup>lec-</sup>) (Figure 5A and B). PXB mice received either the vehicle (the histidine buffer described earlier) every other day for 11 total doses, AvFc at 25 mg/kg every

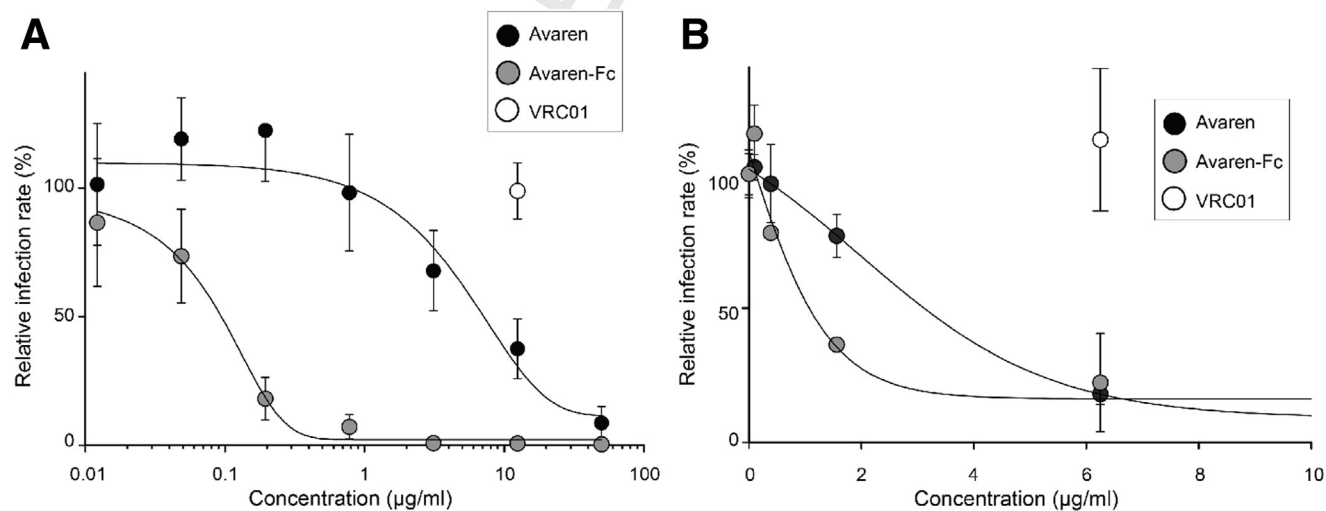


**Figure 1. In vitro HCV inhibition assays.** (A) Avaren and AvFc inhibit cell-culture derived HCV. The JFH1 virus was preincubated with Avaren, AvFc, or the control antibody VRC01 for 30 minutes at 37°C before incubation with Huh-7 cells. At 48 hours after infection, infected cells were quantified by indirect immunofluorescence with an HCV-specific antibody. Results are expressed as a percentage of infection compared with a control infection in the absence of compound. Error bars indicate SEM values from at least 3 independent experiments. (B) Avaren and AvFc inhibit HCV entry. Retroviral pseudotypes bearing HCV envelope glycoproteins of the JFH1 virus (HCVpp) were preincubated with Avaren, AvFc, or the control antibody VRC01 for 30 minutes at 37°C before incubation with Huh-7 cells. At 48 hours after infection, cells were lysed to quantify the luciferase activity. Results are expressed as the percentage of infection compared with the control infection in the absence of compound. Error bars indicate SEM values from at least 3 independent experiments.

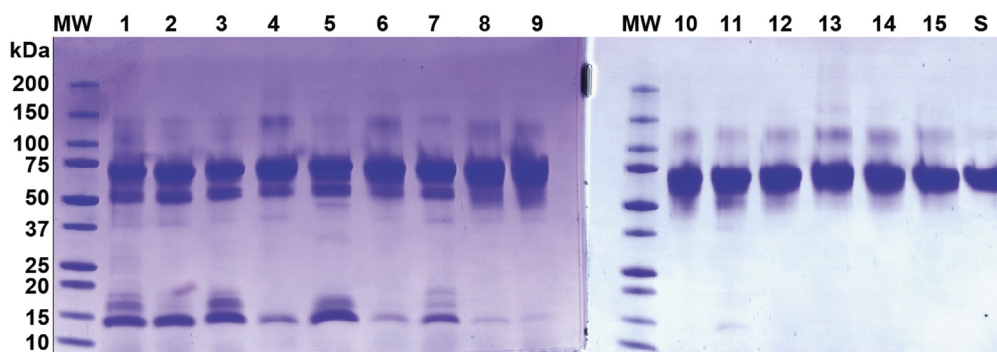


**Figure 2. Stability of AvFc in various buffers.** The initial buffer screening was performed by incubating 1 mg/mL of AvFc at 37°C for 2 weeks in various buffers without any excipient (listed in Table 2), followed by sodium dodecyl sulfate–polyacrylamide gel electrophoresis analysis. The image shows a Coomassie Brilliant Blue–stained gel resolving 10 µg of AvFc from respective buffers, including glutamate at pH 4.5 (lane 1) and 5.0 (lane 2); acetate at pH 4.5 (lane 3) and 5.5 (lane 4); citrate at pH 5.0 (lane 5) and 6.0 (lane 6); succinate at pH 5.5 (lane 7) and 6.5 (lane 8); histidine at pH 6.0 (lane 9) and 7.0 (lane 10); phosphate at pH 6.5 (lane 11), 7.0 (lane 12), and 7.5 (lane 13); Tris at pH 7.5 (lane 14); and PBS (lane 15). At pH 6.0 and less (buffers 1–9), AvFc showed significant degradation after 2 weeks at 37°C. AvFc did not significantly degrade in buffers 10–15, and therefore these were chosen for further preformulation analysis. MW, molecular weight marker; S, standard AvFc control.

other day for a total of 8 or 11 doses, or AvFc<sup>lec-</sup> at 25 mg/kg every other day for 11 total doses. As shown in Figure 6A–C, no significant differences in either body weights, blood h-Alb levels, or serum alanine aminotransferase (ALT) activity were observed. In addition, no significant differences in relative liver weight were seen (Figure 6D). These results indicate that AvFc, formulated in the histidine buffer, was well tolerated in the immunocompromised mice engrafted with human hepatocytes.

Histopathology was performed to evaluate any potential toxicity to the human liver grafts resulting from AvFc administration (Table 3 and Figure 7). In the human hepatocyte area, a slight to moderate (scores of 2–3 in Table 2) macrovesicular fatty change, a characteristic change of

human hepatocytes in the PXB mouse, was observed in all mice, including the vehicle-treated group (Figure 7A–C). Minimal inflammatory cell infiltration around vacuolated hepatocytes (score, 1) was seen in 1 mouse each from the 11-dose AvFc and AvFc<sup>lec-</sup> groups (Figure 7D and E); however, this was unlikely treatment-related because a similar change is seen occasionally in PXB mice (PhoenixBio, New York, NY) (unpublished observation). No AvFc treatment-specific change was observed, except for an incidental build-up of pigmentation found in the Glisson's sheath in the liver of 1 mouse (Figure 7F). Collectively, it was concluded that there was no treatment-related adverse effect in the liver tissue. The full pathology report may be found in the Supplementary Information.

**Table 2. Buffers Used in the Initial Screening of AvFc Preformulation Analysis**

Number	Formulation	pH
1	30 mmol/L glutamate (5.61 g/L NaOOCCH <sub>2</sub> CH <sub>2</sub> CH(NH <sub>2</sub> )COOH × H <sub>2</sub> O) <sup>a</sup>	4.5
2	30 mmol/L glutamate (5.61 g/L NaOOCCH <sub>2</sub> CH <sub>2</sub> CH(NH <sub>2</sub> )COOH × H <sub>2</sub> O) <sup>a</sup>	5.0
3	30 mmol/L acetate (2.46 g/L CH <sub>3</sub> COONa) <sup>a</sup>	4.5
4	30 mmol/L acetate (2.46 g/L CH <sub>3</sub> COONa) <sup>a</sup>	5.5
5	30 mmol/L citrate (350 mL 0.1 mol/L C <sub>6</sub> H <sub>8</sub> O <sub>7</sub> × H <sub>2</sub> O, 650 mL 0.1 mol/L C <sub>6</sub> H <sub>5</sub> O <sub>7</sub> Na <sub>3</sub> × 2 H <sub>2</sub> O)	5.0
6	30 mmol/L citrate (115 mL 0.1 mol/L C <sub>6</sub> H <sub>8</sub> O <sub>7</sub> × H <sub>2</sub> O, 885 mL 0.1 mol/L C <sub>6</sub> H <sub>5</sub> O <sub>7</sub> Na <sub>3</sub> × 2 H <sub>2</sub> O)	6.0
7	30 mmol/L succinate (4.86 g/L NaOOCCH <sub>2</sub> CH <sub>2</sub> COONa) <sup>a</sup>	5.5
8	30 mmol/L succinate (4.86 g/L NaOOCCH <sub>2</sub> CH <sub>2</sub> COONa) <sup>a</sup>	6.5
9	30 mmol/L histidine (4.65 g/L C <sub>6</sub> H <sub>9</sub> N <sub>3</sub> O <sub>2</sub> ) <sup>a</sup>	6.0
10	30 mmol/L histidine (4.65 g/L C <sub>6</sub> H <sub>9</sub> N <sub>3</sub> O <sub>2</sub> ) <sup>a</sup>	7.0
11	30 mmol/L phosphate (2.89 g/L NaH <sub>2</sub> PO <sub>4</sub> × H <sub>2</sub> O, 2.42 g Na <sub>2</sub> HPO <sub>4</sub> × 7 H <sub>2</sub> O)	6.5
12	30 mmol/L phosphate (1.75 g/L NaH <sub>2</sub> PO <sub>4</sub> × H <sub>2</sub> O, 4.64 g Na <sub>2</sub> HPO <sub>4</sub> × 7 H <sub>2</sub> O)	7.0
13	30 mmol/L phosphate (0.78 g/L NaH <sub>2</sub> PO <sub>4</sub> × H <sub>2</sub> O, 6.53 g Na <sub>2</sub> HPO <sub>4</sub> × 7 H <sub>2</sub> O)	7.5
14	30 mmol/L Tris (3.63 g/L NH <sub>2</sub> C(CH <sub>2</sub> OH) <sub>3</sub> ) <sup>a</sup>	7.5
15	PBS (0.144 g/L KH <sub>2</sub> PO <sub>4</sub> , 9 g/L NaCl, 0.795 g/L Na <sub>2</sub> HPO <sub>4</sub> )	7.2

<sup>a</sup>pH was adjusted with 1 mol/L NaOH or 1 mol/L HCl.

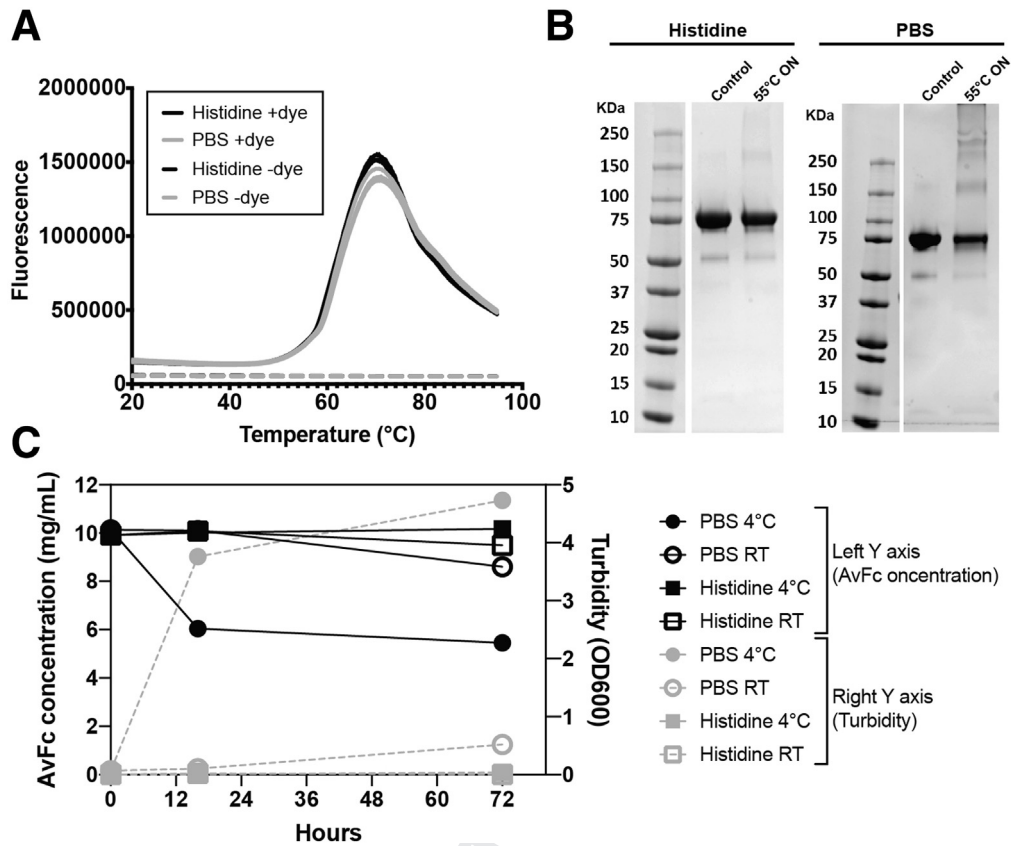


**Figure 3. Liquid formulation development for AvFc.** (A) Differential scanning fluorimetry for melting temperature measurement. AvFc was prepared in 30 mmol/L histidine buffer, 100 mmol/L NaCl, 100 mmol/L sucrose (histidine, *black line*), or PBS (grey line) at a concentration of 1 mg/mL and analyzed in triplicate in the presence (*solid line*) or absence (*dashed line*) of the fluorescent dye SYPRO Orange. Melting temperature values were  $62.49^{\circ}\text{C} \pm 0.13^{\circ}\text{C}$  in the histidine buffer and  $62.68^{\circ}\text{C} \pm 0.25^{\circ}\text{C}$  in PBS, as determined by the vertex of the first derivative of the relative fluorescence unit values. (B) Accelerated stability testing of AvFc in the histidine buffer and PBS. AvFc, prepared at 1 mg/mL in the histidine buffer or PBS were incubated overnight at  $55^{\circ}\text{C}$ , and 10  $\mu\text{g}$  of the protein from each formulation was analyzed by sodium dodecyl sulfate–polyacrylamide gel electrophoresis under nonreducing conditions. A representative Coomassie-stained gel image is shown. The band at around 75 kilodaltons corresponds to AvFc. Note that after overnight incubation, PBS shows less band intensity for AvFc and more large-size aggregate bands than the histidine buffer. (C) Time course of concentration change and the turbidity of AvFc solution in the histidine buffer and PBS. AvFc was formulated at 10 mg/mL in respective buffers and incubated at  $4^{\circ}\text{C}$  or room temperature (RT). After 16 and 72 hours, the concentration was measured using a theoretical extinction coefficient at 280 nm of  $1.6493 (\text{mg/mL})^{-1} \text{cm}^{-1}$ , whereas turbidity was assessed by absorbance at 600 nm. Representative data are shown for samples analyzed in triplicate.

### AvFc Protects Against HCV Infection In Vivo

Lastly, we assessed the protective efficacy of AvFc against HCV infection in vivo using the treatment regimen described earlier. PXB mice were inoculated intraperitoneally with a genotype 1a virus along with initial treatment with 25 mg/kg of AvFc or AvFc<sup>lec-</sup> on day 0. As shown in Figure 8A, AvFc<sup>lec-</sup>-treated mice showed high serum HCV RNA levels from day 7 after challenge through the end of the study on day 35. In sharp contrast, animals treated with both 8 and 11 doses of AvFc did not show any quantifiable level ( $4.0 \times 10^4$  copies/mL) of HCV RNA in sera, indicating that the lectin prevented the infection of human liver grafts by the virus. Similar to the results in Figure 3, overall no major toxicity signal was noted in body weights, human albumin (h-Alb), or h-ALT levels between the test groups, although there was a temporal decrease in body weight and

h-Alb in 1 of the AvFc-treated groups at an early time point, indicating that the liver grafts remained functional over the course of the study (Figure 8B–D).

### Discussion

In this study we showed that the HMG-binding lectin AvFc shows broad genotype-independent anti-HCV activity. In addition, systemic administration of AvFc effectively protected chimeric human-mouse liver mice from infection with a genotype 1a virus without apparent toxicity, providing in vivo proof-of-concept for the lectin's antiviral potential.

The mechanism of HCV neutralization by AvFc likely is through binding to HMGs on the E1/E2 envelope protein dimer, which blocks their interaction with host cell

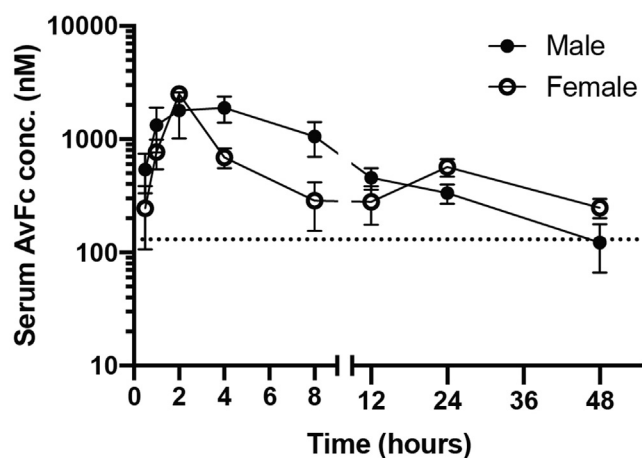


**Figure 4. Pharmacokinetics of AvFc in mice.** AvFc pharmacokinetics were evaluated in C57bl/6 mice after a single intraperitoneal injection of 25 mg/kg with blood sampled at various time points. Data are expressed as means  $\pm$  SEM from 4 mice per group. The average half-life was 24.5 and 18.5 hours in male and female mice, respectively, as determined by the PKSolver Microsoft Excel Add-on. The peak concentration occurred between 2 and 4 hours after administration. The target trough concentration of 130 nmol/L (corresponding to 10  $\mu$ g/mL) is indicated by a dashed line.

receptors and viral entry. Unlike HIV envelope glycoproteins, whose glycan content can vary widely between strains, the number and position of glycosylation sites on E1/E2 are highly conserved, indicating their critical role in HCV's infectious processes.<sup>27</sup> The notion that AvFc functions as an entry inhibitor is supported by the fact that the lectin body has affinity to the E2 protein<sup>24</sup> and that other mannose-binding lectins, such as Griffithsin or Cyanovirin-N, inhibit entry in this manner.<sup>28,29</sup> AvFc inhibited multiple genotypes of HCV with average 50% inhibitory concentrations more than 100-fold lower than that of the monomer Avaren lectin (Table 1), indicating that the multivalent recognition of HMGs on the surface of the virus, brought about by the dimerization of Avaren via Fc fusion, led to greater entry inhibition. Unlike other antiviral lectins, however, the inclusion of the human IgG1 Fc region implicates the possibility of Fc-mediated effector functions, such as antibody-dependent cell-mediated cytotoxicity, against infected cells. In fact, Fc-mediated effector functions greatly contributed to the antiviral potency of AvFc against HIV, as determined by a primary cell-based inhibition assay and an antibody-dependent cell-mediated viral inhibition assay.<sup>24</sup> Accordingly, the remarkable efficacy seen in the present *in vivo* HCV challenge study may be partially Fc-mediated. Further investigations are necessary to address this possibility.

The present study also showed that AvFc therapy is well tolerated in mice and human hepatocytes because every-other-day intraperitoneal administration of 25 mg/kg AvFc, of up to 11 doses, did not show any obvious toxicity in PXB mice by gross necropsy or histopathology of engrafted human hepatocytes, and it did not result in significant changes in body weight, h-Alb level, or ALT level (Figures 6

and 7). This corroborates our previous observation that AvFc administration, both intraperitoneally and intravenously, was well tolerated and produced no toxicity in mice, rats, or rhesus macaques.<sup>24</sup> We hypothesize that the lack of any significant toxicity is attributable to the unique HMG-binding mechanism of AvFc, whereby it requires multivalent interaction with several HMGs in proximity to show high-affinity binding to a glycoprotein target. In line with this hypothesis, Hoque et al<sup>30</sup> showed that the 3 binding pockets of the parent lectin actinohivin can bind up to 3 independent HMGs, providing high-affinity binding when the HMGs are in relatively close proximity. This implies that AvFc may not interact effectively with healthy normal cells and tissues that do not usually show clusters of HMGs on their surfaces. In contrast, glycoproteins of many enveloped viruses show a high proportion of these immature forms of *N*-glycans.<sup>20–22</sup> Although HCV E2 has fewer *N*-glycosylation sites (approximately 11) than the HIV gp120 (which has between 20 and 30, depending on the strain), E2 likely is present on the surface of HCV at a higher density and thus provides higher local concentrations of HMGs.<sup>31</sup> Further studies are necessary to show a threshold HMG concentration that enables efficient interaction between AvFc and the surfaces of cells or viruses.

Although alcoholic liver disease has now surpassed HCV infection as the number one indication for liver transplantation in the United States, a large number of procedures will continue to be performed for the foreseeable future in patients with HCV-related decompensated cirrhosis.<sup>32</sup> A major outstanding issue is the lack of effective treatment protecting the allograft liver from recurrent infection by the virus that remained circulating in the periphery at the time of transplant. As a consequence, re-infection of donor livers occurs universally, as early as in the first 90 minutes of reperfusion,<sup>17</sup> and can result in accelerated fibrosis and increased risk of graft failure, cirrhosis, and hepatocellular carcinoma.<sup>33</sup> In fact, allograft failure resulting from re-infection is the leading cause of secondary transplants and death in HCV-infected patients who have received a liver transplant.<sup>34</sup> Patients cured of HCV with DAAs after liver transplantation still have a higher-than-normal risk of hepatocellular carcinoma,<sup>35</sup> and the high cost of the drugs represents a significant barrier to their widespread use. Furthermore, emergent drug resistance, even in DAA combination therapies, although rare, represents a particular challenge for further treatment.<sup>36</sup> Unlike DAAs, entry inhibitors neutralize circulating viruses and physically block the viral infection of target cells. The use of entry inhibitors perioperatively upon liver transplantation, either alone or in combination with DAAs, may improve treatment outcomes significantly.<sup>34,37</sup> Thus, although the effectiveness of DAAs is not in question, there still are unmet needs that may be addressed through the use of entry inhibitors.

To date, no entry inhibitor has been approved for the treatment or prevention of HCV. Two major drug candidates, Civacir and MBL-HCV1, have shown some promise in clinical trials (NCT01804829 and NCT01532908).<sup>38,39</sup> Although larger studies are needed, it appears that entry

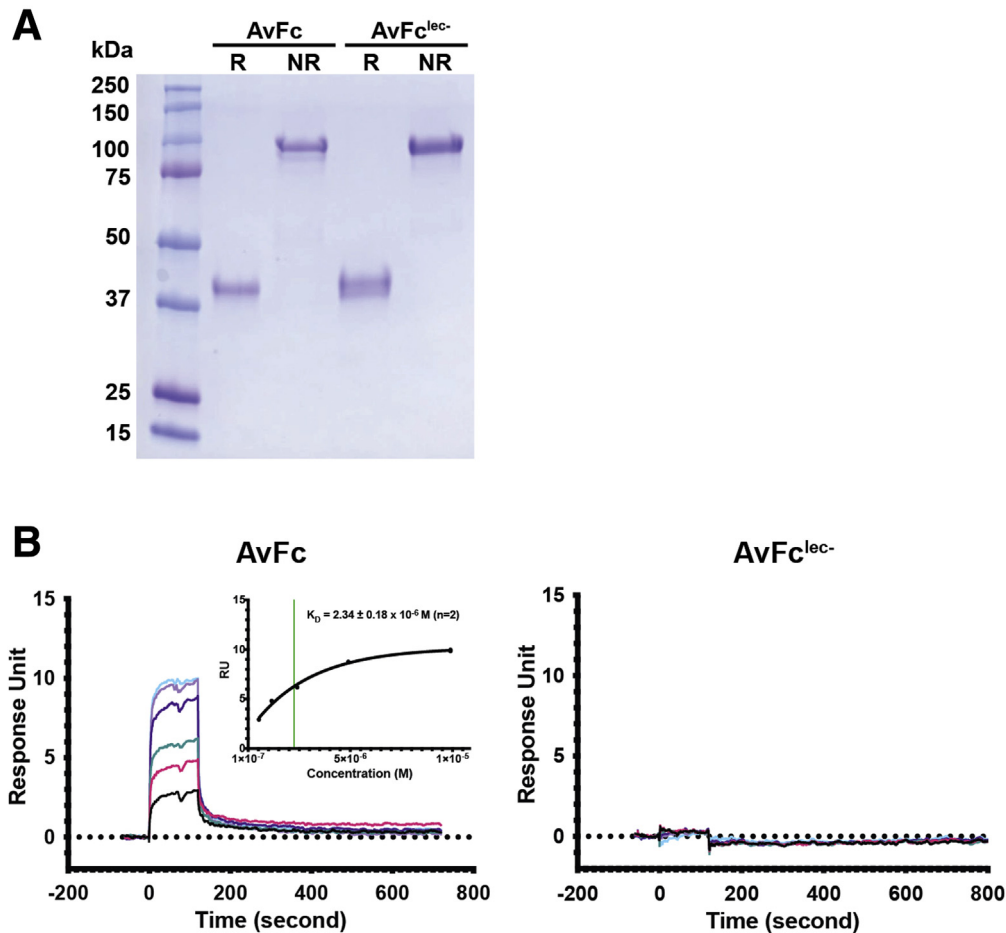


**Figure 5. Characterization of the non-sugar-binding mutant AvFc<sup>lec-</sup>.** A variant of AvFc that does not bind to HMGs was generated by mutating a tyrosine residue in each of the 3 binding pockets of Avaren (Dent et al, unpublished data). (A) Sodium dodecyl sulfate-polyacrylamide gel electrophoresis showing purified AvFc and AvFc<sup>lec-</sup> under reducing (R) and nonreducing (NR) conditions. Under R conditions, AvFc monomer is seen at 38.5 kilodaltons; under NR conditions, AvFc dimer (via interpeptide disulfide bonds in the Fc region) appears at 77 kilodaltons. (B) Surface plasmon resonance analysis of HCV E2-binding affinity of AvFc and AvFc<sup>lec-</sup>. A recombinant E2 protein (Immune Technology Corp) was immobilized to a CM5 chip using amine coupling to a surface density of approximately 200 response units (RU). AvFc or AvFc<sup>lec-</sup> then was injected over the chip surface at a rate of 30  $\mu\text{L}/\text{min}$  for 120 seconds, followed by a 600-second dissociation period, with concentrations ranging from 10 to 0.625  $\mu\text{mol}/\text{L}$ . Binding affinity was calculated using steady-state analysis and was determined to be  $2.34 \pm 0.18 \times 10^{-6} \text{ mol}/\text{L}$  ( $2.34 \pm 0.18 \mu\text{mol}/\text{L}$ ) for AvFc. Binding affinity could not be determined for AvFc<sup>lec-</sup> because of the lack of measurable binding.

inhibitors in combination with DAAs may represent a new treatment paradigm for HCV patients receiving a liver transplant. Despite both MBL-HCV1 and Civacir being capable of neutralizing a broad range of HCV genotypes, viral resistance still can develop through mutations in the envelope proteins E1/E2, in particular through shifting glycan positions.<sup>40,41</sup> In this regard, AvFc in its own right could be less susceptible to amino acid mutations because it targets the glycan shield of the virus rather than a specific epitope. Deletions of glycans, even if occurring after prolonged exposure to a carbohydrate-binding agent such as AvFc, may result in a significant decrease in viral fitness by decreasing E1/E2 incorporation into HCV particles or increased susceptibility to humoral immunity resulting from a breach in the glycan shield.<sup>27,42</sup> Our results provide a foundation to test the earlier-described hypotheses and

feasibility of the HMG-targeting anti-HCV strategy. Of note, a unique advantage of AvFc over the 2 antibody-based entry inhibitor candidates described earlier is that the lectin body has the capacity to neutralize both HIV<sup>24</sup> and HCV (present study). Accordingly, AvFc may provide an effective means (eg, pre-exposure prophylaxis) to protect high-risk populations against HIV/HCV co-infection, such as health care workers and injection drug users.<sup>43,44</sup>

In conclusion, the present study provides an important proof of concept for the therapeutic potential of AvFc against HCV infection via targeting envelope HMGs. In particular, the lectin body may provide a safe and efficacious means to prevent recurrent infection on liver transplantation in HCV-related end-stage liver disease patients. Other potential utilities of AvFc may be found in pre-exposure prophylaxis against HIV/HCV co-infection



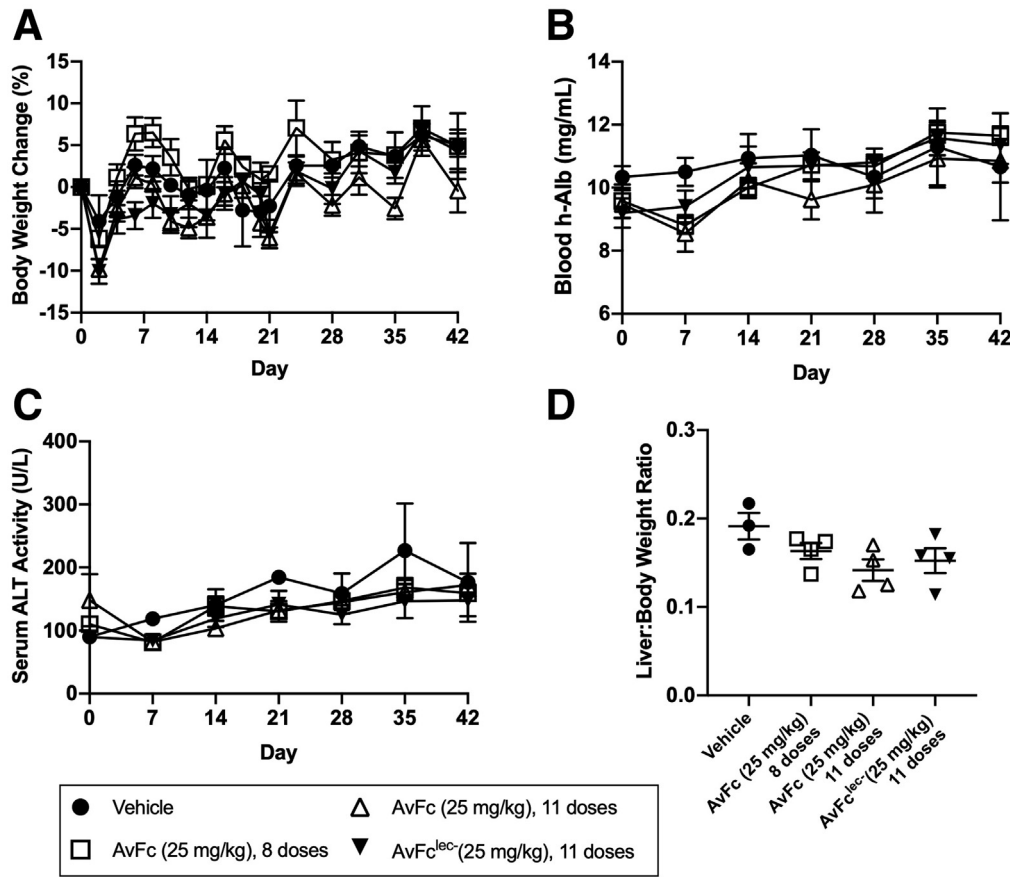


**Figure 6.** Toxicologic analysis of systemically administered AvFc in the PXB human liver chimeric mouse model. PXB mice were administered AvFc or AvFc<sup>lec</sup> intraperitoneally at 25 mg/kg (n = 4 each), or the histidine buffer vehicle control (n = 3) every 2 days and monitored for body weight, blood h-Alb level, and serum alanine ALT level over 42 days. (A) Percentage change of body weights from the initial day of dosing (day 0). (B) Blood h-Alb levels. (C) Serum ALT levels. (D) Ratio of liver weight to body weight of individual mice at necropsy. (A–C) Each data point represents means ± SEM and (D) individual data with means ± SEM in each group. No significant changes in any of the safety end points were noted between the groups (A–C, 2-way analysis of variance; D, 1-way analysis of variance).

high-risk populations, as well as in the context of transplantation of organs from HCV-infected donors to HCV-negative recipients, which may help alleviate the severe shortage of donor organs available for transplantation.<sup>45,46</sup> Further studies are warranted to determine a dose-response relationship, therapeutic window, and feasibility of intravenous or subcutaneous dosing routes, as well as to assess the efficacy of AvFc against established infection.

**Materials and Methods**

*Animal Care*

The use of animals was approved by the University of Louisville’s Institutional Animal Care and Use Committee and the Animal Ethics Committee of PhoenixBio Company, Ltd (resolution 2281). All animals were given a standard diet and water ad libitum and were housed in a temperature- and humidity-controlled facility with a 12-hour day/night cycle.

**Table 3.** Histopathology of Chimeric Mouse Liver Tissue

	Vehicle			AvFc <sup>lec</sup>				AvFc, 11 doses				AvFc, 8 doses			
	101	102	103	201	202	203	204	301	302	303	304	401	402	403	404
Mouse hepatocytes	0	0	0	0	0	0	0	0	0	0	0	0	0	0	0
Human hepatocytes	2	3	3	3	3	3	3	3	3	3	3	3	3	3	3
Fatty change, macrovesicular															
Infiltrate, inflammatory cell, around vacuolated hepatocyte	0	0	0	0	1	0	0	0	1	0	0	0	0	1	0
Portal canal and others															
Hepatocellular carcinoma, trabecular, with extramedullary hematopoiesis	P	0	0	0	0	0	0	0	0	0	0	0	0	0	0
Metaplasia, osseous	0	2	0	0	0	0	0	0	0	0	0	0	0	0	0
Pigmentation, brown, histiocyte, Glisson sheath, focal	0	0	0	0	0	0	0	0	0	0	0	1	0	0	0

NOTE. Numbers shown are the severity score on a scale of 0–5. P, present.

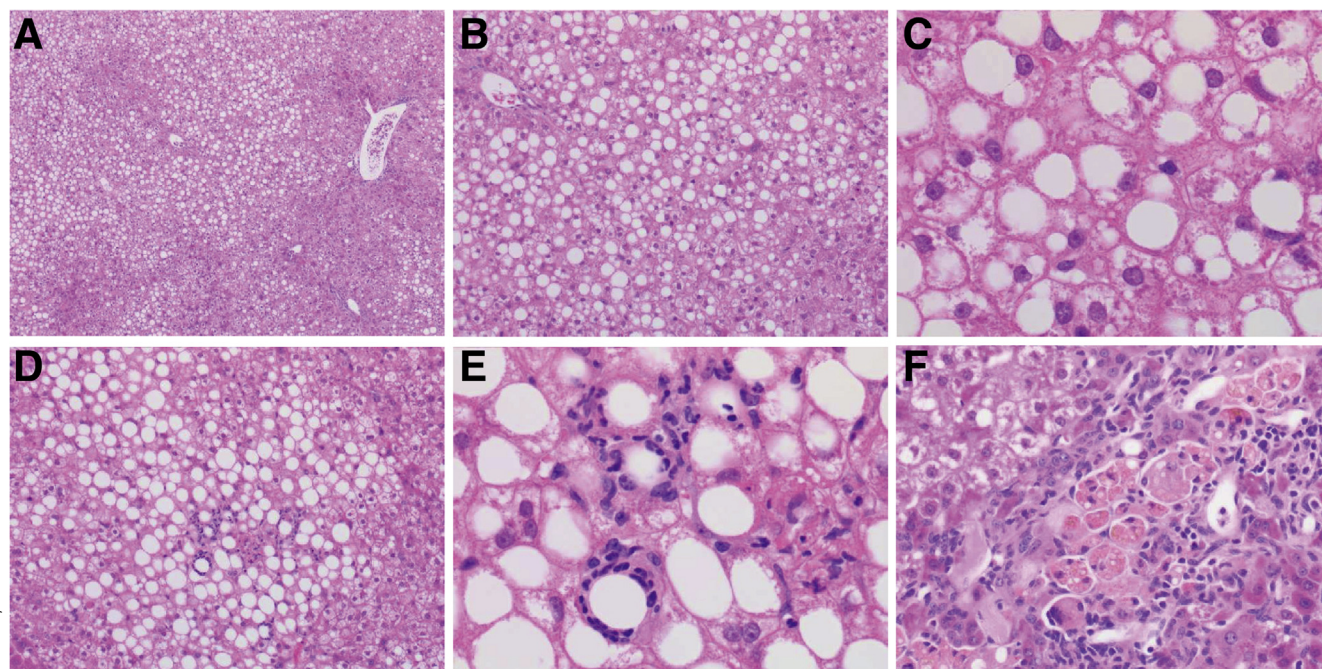


**Figure 7. Histopathologic examination of PXB mouse liver tissues.** Representative H&E-stained liver tissue section images corresponding to histopathologic findings in Table 2 are shown. Liver tissues are from the toxicologic study in Figure 4. (A) A 4× image from an animal in the vehicle control group (mouse ID: 103 in Table 2) showing low magnification of vacuolated hepatocytes. (B) A 10× image from a portion of panel A, containing many human hepatocytes with a large, well-defined, rounded vacuole. (C) Higher magnification (40×) of panel B. (D) A 10× image from an animal in the AvFc<sup>lec-</sup> group (ID: 202 in Table 2), showing small foci of inflammatory cell inflammation in the human hepatocyte area. (E) Higher magnification (40×) of panel D. Inflammatory cells appear to surround vacuolated hepatocytes. (F) A 20× image from an animal in the AvFc group (8 total doses; ID: 401 in Table 2). Histiocytic brown pigmentation in the Glisson sheath was noted only in this mouse.

### Production of AvFc and Non-HMG-Binding AvFc Variant

AvFc and AvFc<sup>lec-</sup> were produced by agroinfiltration with magnICON vectors in *Nicotiana benthamiana* plants as previously described.<sup>24</sup> AvFc was purified from plants after a 7-day incubation period using protein A and ceramic hydroxyapatite chromatography.

### HCV Neutralization Assays

Huh-7 cells<sup>47</sup> and HEK-293T cells (American Type Culture Collection, Manassas, VA) were cultured in Dulbecco's modified Eagle medium supplemented with 10% heat-inactivated fetal calf serum and 1% penicillin/streptomycin. To produce HCVcc, we used a modified version of the plasmid encoding JFH1 genome (genotype 2a), provided by T. Wakita (National Institute of Infectious Diseases, Tokyo, Japan).<sup>48,49</sup> The H77/JFH1 chimera, which expresses the core-NS2 segment of the genotype 1a polypeptide within a genotype 2a background, has been described previously.<sup>50</sup> The genotype 4a ED43/JFH1,<sup>51</sup> genotype 5a SA13/JFH1,<sup>52</sup> and genotype 6a HK6a/JFH1<sup>53</sup> infectious HCV recombinants were provided by J. Bukh (University of Copenhagen, Copenhagen, Denmark). Retroviral pseudotypes bearing HCV envelope glycoproteins of JFH1 virus (HCVpp) expressing the *Firefly* luciferase reporter gene were produced in HEK-293T as previously

described.<sup>54</sup> Inhibitory effects were determined by quantifying infectivity by indirect immunofluorescence with the anti-E1 monoclonal antibody A4<sup>55</sup> or an anti-NS5A polyclonal antibody kindly provided by M. Harris (University of Leeds, Leeds, UK).

### Formulation Buffer Optimization

Initial buffer screening was performed in 30 mmol/L glutamate, acetate, citrate, succinate, histidine, and phosphate buffers at pH 4.5–7.5 (Table 2). All the buffer agents were purchased from MilliporeSigma. AvFc was diafiltrated and adjusted to 1 mg/mL (or 62.5 μmol/L) in respective buffers. Stability was evaluated by sodium dodecyl sulfate–polyacrylamide gel electrophoresis after incubation for 2 weeks at 37°C. The melting temperatures of AvFc were determined by differential scanning fluorimetry performed on an Applied Biosystems StepOnePlus reverse-transcription polymerase chain reaction (RT-PCR) system as described previously.<sup>24</sup> Briefly, AvFc formulated in various buffers at a concentration of 50 μmol/L was mixed with a final concentration of 50× SYPRO Orange (S6651; ThermoFisher Scientific) in a 96-well template. The melting temperature was determined by the vertex of the first derivative of the relative fluorescence unit values in the melt curves. AvFc formulated into the optimized histidine buffer or PBS then was concentrated to 10 mg/mL and incubated

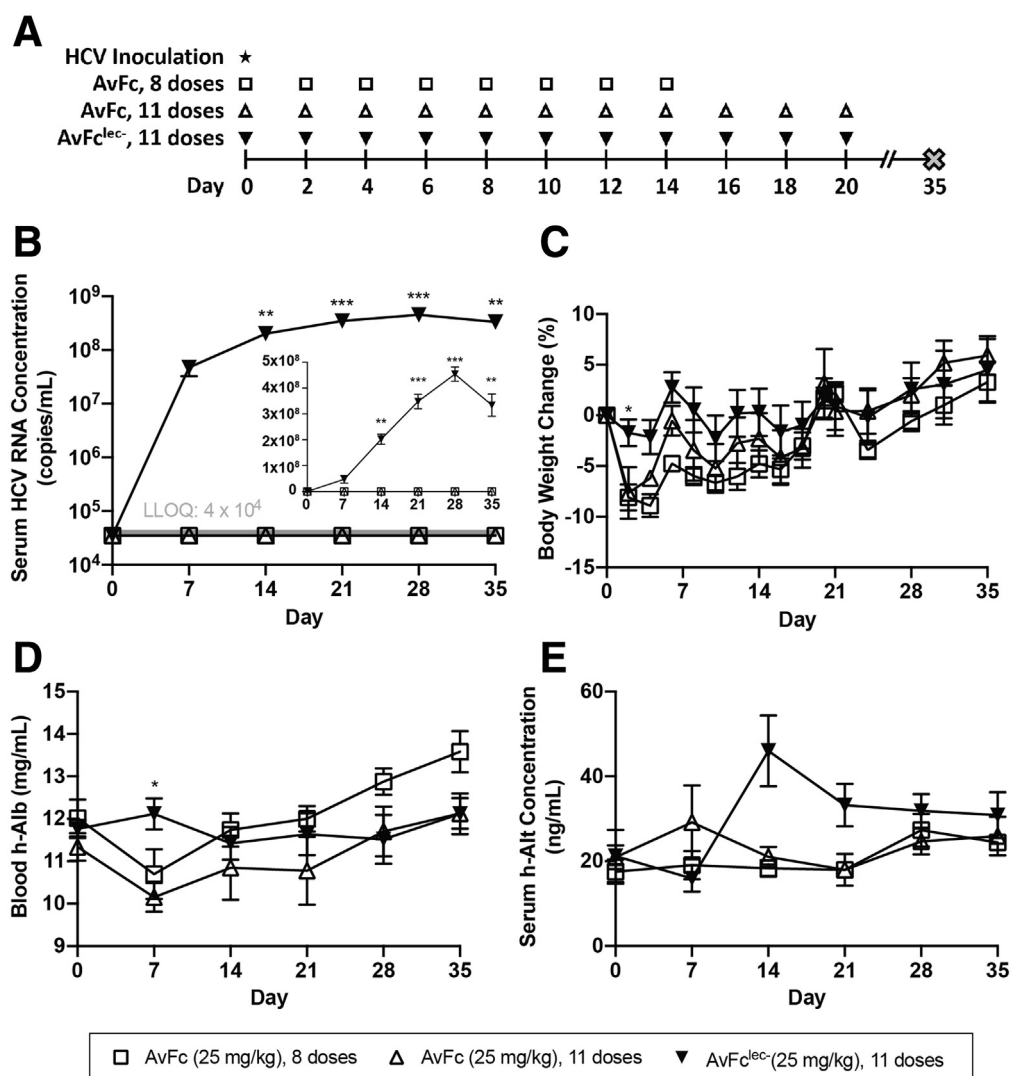


**Figure 8. The protective effect of AvFc against HCV challenge in PXB mice.** (A) Study design. PXB mice were challenged intraperitoneally with a HCV genotype 1a virus on day 0, simultaneously with an initial treatment intraperitoneally with either 25 mg/kg of AvFc or AvFc<sup>lec-</sup>. Treatment was continued every other day for a total of 8 or 11 doses for AvFc and 11 doses for AvFc<sup>lec-</sup> (n = 5 each). The general conditions and body weights of the animals were monitored every other day, while serum HCV RNA and blood h-Alb levels were measured every 7 days. (B) Serum HCV RNA levels. AvFc treatment (both 8 and 11 doses) showed no detectable HCV RNA at any time point. The gray line indicates the lower limit of quantification, which was 4 × 10<sup>4</sup> copies/mL in this assay. \*\*P < .01, \*\*\*P < .001 (AvFc<sup>lec-</sup> vs both AvFc 8 and 11 doses); 2-way analysis of variance with the Tukey multiple comparison test. Inset: The graph shows the same data with the y-axis on a linear scale. (C–E) Time course of body weight change from day 0 (C), blood h-Alb levels (D), and serum h-Alt concentrations (E). Each data point represents means ± SEM in each group. \*P < 0.05 (C, AvFc<sup>lec-</sup> vs AvFc 8 doses; D, AvFc<sup>lec-</sup> vs AvFc 11 doses; 2-way analysis of variance with the Tukey multiple comparison test. (E) No significant difference between groups at any time point was noted.

at 4°C or room temperature. Absorbance at 280 nm and 600 nm was measured immediately after concentration and then again after 16 and 72 hours. A<sub>280</sub> was measured after centrifugation of precipitate.

### Pharmacokinetic Analysis

A pharmacokinetic profile for AvFc was generated after a single 25-mg/kg intraperitoneal injection in C57bl/6 mice (The Jackson Laboratory, Bar Harbor, ME) (8-week-old males and females; n = 4 per time point) and sampling blood at 0.5, 1, 2, 4, 8, 12, 24, and 48 hours after injection.

The concentration of AvFc then was measured using an HIV gp120-coated enzyme-linked immunosorbent assay. Briefly, a recombinant gp120 (HIV CM235; AIDS Reagent Program; National Institutes of Health, Bethesda, MD) was coated overnight at 0.3 μg/mL followed by blocking with 5% dry milk-PBST. Serum samples at varying dilutions were incubated for 2 hours, followed by detection by a goat anti-human Fc-horseradish-peroxidase secondary antibody (ThermoFisher Scientific). The plasma concentration of AvFc was calculated by interpolating from a standard curve. PK parameters were calculated using the PKSolver Microsoft Excel add-on.<sup>56</sup>

## 1179 *Toxicologic Analysis and HCV Challenge Study in* 1180 *PXB Mice*

1181 The mouse model of toxicologic analysis and HCV  
1182 infection and toxicologic analysis was performed in PXB  
1183 mice (complementary DNA-uPA<sup>wild/+</sup>/SCID, complemen-  
1184 tary DNA-uPA<sup>wild/+</sup>: B6; 129SvEv-Plau, SCID: C.B-17/Icr-  
1185 scid/scid Jcl; reviewed by Tateno and Kojima<sup>25</sup>). These mice  
1186 contain transplanted human hepatocytes with a replace-  
1187 ment index of greater than 70% as determined by blood h-  
1188 Alb measurements before virus inoculation.<sup>57</sup> Blood h-Alb  
1189 levels indicate the level and integrity of human hepatocyte  
1190 engraftment in the mouse liver. Mice were separated into  
1191 the following 3 treatment groups: AvFc<sup>lcc</sup> (25 mg/kg, n = 5)  
1192 for 11 doses, or AvFc (25 mg/kg, n = 5 each) for 8 or 11  
1193 doses. The initial treatment was co-administered intraperi-  
1194 toneally with virus inoculation ( $5 \times 10^5$  copies/kg) on day  
1195 0 with a genotype 1a strain (PBC002), and treatment  
1196 continued every other day thereafter. The general condi-  
1197 tions and body weights of the animals were monitored  
1198 every other day, while serum HCV RNA and blood h-Alb  
1199 were measured every 7 days by RT-PCR or latex aggluti-  
1200<sup>q29</sup> nation immunonephelometry (LZ Test Eiken U-ALB; Eiken  
1201 Chemical Co, Ltd), respectively. The HCV RNA RT-PCR assay  
1202 was developed based on the method described by Takeuchi  
1203 et al<sup>58</sup> with modifications, and validated by PhoenixBio for  
1204 use in this animal model. The lower limit of quantification  
1205 was determined to be  $4.0 \times 10^4$  copies/mL. Serum ALT 1  
1206 levels were determined either using a Fujifilm DRI-CHEM  
1207 NX500sV clinical chemistry instrument or by enzyme-  
1208 linked immunosorbent assay (Institute of Immunology Co,  
1209 Ltd, Tokyo, Japan). At study termination on day 35, animals  
1210 were killed and subject to gross necropsy and general  
1211<sup>q30</sup> health. Blood also was drawn via cardiac puncture and used  
1212 for ALT, HCV RNA, and h-Alb analyses.

## 1213 *Histopathologic Analysis of Liver Tissues*

1214 H&E-stained liver sections from 3 to 4 mice per group  
1215 were generated by Nara Pathology Research Institute Co,  
1216 Ltd (Nara, Japan) and evaluated by pathologists at SkyPatho,  
1217 LLC. All slides were examined by a blinded, board-certified  
1218<sup>q31</sup> veterinary pathologist under a light microscope (BX43;  
1219 Olympus Corporation, Tokyo, Japan). The tissues were  
1220 assigned a severity score for a number of characteristics  
1221 based on the 5-point scoring system of the CDISC SEND  
1222<sup>q32</sup> Controlled Terminology, as follows: 0, unremarkable; 1,  
1223 minimal; 2, mild; 3, moderate; 4, marked; 5, severe; and P,  
1224 present.

## 1225 *Statistical Analyses and Data Analysis*

1226 Statistical significance was analyzed by GraphPad Prism  
1227 6 software (La Jolla, CA). Mouse body weights, albumin, ALT,  
1228 and HCV RNA levels were compared using a repeated-  
1229 measures 2-way analysis of variance with the  
1230 Geisser-Greenhouse correction. Multiple comparisons be-  
1231 tween groups at each time point were conducted and cor-  
1232 rected using the Tukey method with the threshold of  
1233 significance set at  $P = .05$ . Liver:body-weight ratios were  
1234 compared using 1-way analysis of variance. All authors had

access to the study data, and reviewed and approved the  
final manuscript.

## References

1. Penin F, Dubuisson J, Rey FA, Moradpour D, Pawlotsky JM. Structural biology of hepatitis C virus. *Hepatology* 2004;39:5–19.
2. Blach S, Zeuzem S, Manns M, Altraif I, Duberg A-S, Muljono DH, Waked I, Alavian SM, Lee M-H, Negro F. Global prevalence and genotype distribution of hepatitis C virus infection in 2015: a modelling study. *Lancet Gastroenterol Hepatol* 2017;2:161–176.
3. Zibbell JE, Asher AK, Patel RC, Kupronis B, Iqbal K, Ward JW, Holtzman D. Increases in acute hepatitis C virus infection related to a growing opioid epidemic and associated injection drug use, United States, 2004 to 2014. *Am J Public Health* 2018;108:175–181.
4. Zibbell JE, Iqbal K, Patel RC, Suryaprasad A, Sanders KJ, Moore-Moravian L, Serrecchia J, Blankenship S, Ward JW, Holtzman D. Increases in hepatitis C virus infection related to injection drug use among persons aged  $\leq 30$  years—Kentucky, Tennessee, Virginia, and West Virginia, 2006–2012. *MMWR Morb Mortal Wkly Rep* 2015;64:453.
5. Manns MP, Buti M, Gane E, Pawlotsky J-M, Razavi H, Terrault N, Younossi Z. Hepatitis C virus infection. *Nat Rev Dis Primers* 2017;3:17006.
6. Negro F, Forton D, Craxi A, Sulkowski MS, Feld JJ, Manns MP. Extrahepatic morbidity and mortality of chronic hepatitis C. *Gastroenterology* 2015; 149:1345–1360.
7. Manns MP, McHutchison JG, Gordon SC, Rustgi VK, Shiffman M, Reindollar R, Goodman ZD, Koury K, Ling M-H, Albrecht JK. Peginterferon alfa-2b plus ribavirin compared with interferon alfa-2b plus ribavirin for initial treatment of chronic hepatitis C: a randomised trial. *Lancet* 2001;358:958–965.
8. Jacobson IM, McHutchison JG, Dusheiko G, Di Bisceglie AM, Reddy KR, Bzowej NH, Marcellin P, Muir AJ, Ferenci P, Flisiak R. Telaprevir for previously untreated chronic hepatitis C virus infection. *N Engl J Med* 2011;364:2405–2416.
9. Poordad F, McCone J Jr, Bacon BR, Bruno S, Manns MP, Sulkowski MS, Jacobson IM, Reddy KR, Goodman ZD, Boparai N. Boceprevir for untreated chronic HCV genotype 1 infection. *N Engl J Med* 2011; 364:1195–1206.
10. Asselah T, Kowdley KV, Zadeikis N, Wang S, Hassanein T, Horsmans Y, Colombo M, Calinas F, Aguilar H, de Ledingham V, Mantry PS, Hezode C, Marinho RT, Agarwal K, Nevens F, Elkhashab M, Kort J, Liu R, Ng TI, Krishnan P, Lin C-W, Mensa FJ. Efficacy of glecaprevir/pibrentasvir for 8 or 12 weeks in patients with hepatitis C virus genotype 2, 4, 5, or 6 infection without cirrhosis. *Clin Gastroenterol Hepatol* 2018;16:417–426.
11. Afdhal N, Zeuzem S, Kwo P, Chojkier M, Gitlin N, Puoti M, Romero-Gomez M, Zarski J-P, Agarwal K, Buggisch P. Ledipasvir and sofosbuvir for untreated HCV genotype 1 infection. *N Engl J Med* 2014; 370:1889–1898.

- 1297 12. Feld JJ, Moreno C, Trinh R, Tam E, Bourgeois S, 1356  
 1298 Horsmans Y, Elkhashab M, Bernstein DE, Younes Z, 1357  
 1299 Reindollar RW. Sustained virologic response of 100% in 1358  
 1300 HCV genotype 1b patients with cirrhosis receiving 1359  
 1301 ombitasvir/paritaprevir/r and dasabuvir for 12 weeks. 1360  
 1302 *J Hepatol* 2016;64:301–307. 1361
- 1303 13. Zeuzem S, Ghalib R, Reddy KR, Pockros PJ, Ari ZB, 1362  
 1304 Zhao Y, Brown DD, Wan S, DiNubile MJ, Nguyen B-Y. 1363  
 1305 Grazoprevir–elbasvir combination therapy for treatment- 1364  
 1306 naive cirrhotic and noncirrhotic patients with chronic 1365  
 1307 hepatitis C virus genotype 1, 4, or 6 infection: a ran- 1366  
 1308 domized trial. *Ann Intern Med* 2015;163:1–13. 1367
- 1309 14. Fernández-Carrillo C, Lens S, Llop E, Pascasio JM, 1368  
 1310 Fernández I, Baliellas C, Crespo J, Buti M, Castells L, 1369  
 1311 Romero-Gómez M, Pons C, Moreno JM, Albillos A, 1370  
 1312 Fernández-Rodríguez C, Prieto M, Fernández- 1371  
 1313 Bermejo M, García-Samaniego J, Carrión JA, de la 1372  
 1314 Mata M, Badia E, Salmerón J, Herreros JI, Salcedo M, 1373  
 1315 Moreno JJ, Turnes J, Granados R, Blé M, Calleja JL. 1374  
 1316 Treatment of hepatitis C virus in patients with advanced 1375  
 1317 cirrhosis: always justified? Analysis of the Hepa-C Reg- 1376  
 1318 istry. *J Hepatol* 2016;64:S133. 1377
- 1319 15. Belli LS, Berenguer M, Cortesi PA, Strazzabosco M, 1378  
 1320 Rockenschaub S-R, Martini S, Morelli C, Donato F, 1379  
 1321 Volpes R, Pageaux G-P. Delisting of liver transplant 1380  
 1322 candidates with chronic hepatitis C after viral eradica- 1381  
 1323 tion: a European study. *J Hepatol* 2016;65:524–531. 1382
- 1324 16. Jothamani D, Govil S, Rela M. Management of post liver 1383  
 1325 transplantation recurrent hepatitis C infection with 1384  
 1326 directly acting antiviral drugs: a review. *Hepatol Int* 2016; 1385  
 1327 10:749–761. 1386
- 1328 17. Hughes MG Jr, Tucker WW, Reddy S, Brier ME, Koch D, 1387  
 1329 McClain CJ, Jonsson CB, Matoba N, Chung D. Rate of 1388  
 1330 hepatitis C viral clearance by human livers in human 1389  
 1331 patients: liver transplantation modeling primary infection 1390  
 1332 and implications for studying entry inhibition. *PLoS One* 1391  
 1333 2017;12:e0180719. 1392
- 1334 18. Felmler DJ, Coilly A, Chung RT, Samuel D, Baumert TF. 1393  
 1335 New perspectives for preventing hepatitis C virus liver 1394  
 1336 graft infection. *Lancet Infect Dis* 2016;16:735–745. 1395
- 1337 19. Colpitts CC, Baumert TF. Hepatitis C virus cell entry: a 1396  
 1338 target for novel antiviral strategies to address limitations 1397  
 1339 of direct acting antivirals. *Hepatol Int* 2016;10:741–748. 1398
- 1340 20. Iacob RE, Perdivara I, Przybylski M, Tomer KB. Mass 1399  
 1341 spectrometric characterization of glycosylation of hepa- 1400  
 1342 titis C virus E2 envelope glycoprotein reveals extended 1401  
 1343 microheterogeneity of N-glycans. *J Am Soc Mass* 1402  
 1344 *Spectrom* 2008;19:428–444. 1403
- 1345 21. Walls AC, Tortorici MA, Frenz B, Snijder J, Li W, Rey FA, 1404  
 1346 DiMaio F, Bosch B-J, Veelsler D. Glycan shield and 1405  
 1347 epitope masking of a coronavirus spike protein observed 1406  
 1348 by cryo-electron microscopy. *Nat Struct Mol Biol* 2016; 1407  
 1349 23:899–905. 1408
- 1350 22. Leonard CK, Spellman MW, Riddle L, Harris RJ, 1409  
 1351 Thomas JN, Gregory TJ. Assignment of intrachain dis- 1410  
 1352 sulfide bonds and characterization of potential glyco- 1411  
 1353 sylation sites of the type 1 recombinant human 1412  
 1354 immunodeficiency virus envelope glycoprotein (gp120) 1413  
 1355 expressed in Chinese hamster ovary cells. *J Biol Chem* 1414  
 1990;265:10373–10382. 1415
23. Suga A, Nagae M, Yamaguchi Y. Analysis of protein 1356  
 landscapes around N-glycosylation sites from the PDB 1357  
 repository for understanding the structural basis of N- 1358  
 glycoprotein processing and maturation. *Glycobiology* 1359  
 2018;28:774–785. 1360
24. Hamorsky KT, Kouokam JC, Dent MW, Grooms TN, 1361  
 Husk AS, Hume SD, Rogers KA, Villinger F, Morris MK, 1362  
 Hanson CV, Matoba N. Engineering of a lectin body tar- 1363  
 geting high-mannose-type glycans of the HIV envelope. 1364  
*Mol Ther* 2019;27:2038–2052. 1365
25. Tateno C, Kojima Y. Characterization and applications of 1366  
 chimeric mice with humanized livers for preclinical drug 1367  
 development. *Lab Anim Res* 2020;36:2. 1368
26. Hamorsky KT, Grooms-Williams TW, Husk AS, 1369  
 Bennett LJ, Palmer KE, Matoba N. Efficient single toba- 1370  
 moviral vector-based bioproduction of broadly neutral- 1371  
 izing anti-HIV-1 monoclonal antibody VRC01 in 1372  
*Nicotiana benthamiana* plants and utility of VRC01 in 1373  
 combination microbicides. *Antimicrob Agents Chemother* 1374  
 2013;57:2076–2086. 1375
27. Goffard A, Callens N, Bartosch B, Wychowski C, 1376  
 Cosset F-L, Montpellier C, Dubuisson J. Role of N-linked 1377  
 glycans in the functions of hepatitis C virus envelope 1378  
 glycoproteins. *J Virol* 2005;79:8400–8409. 1379
28. Meuleman P, Albecka A, Belouzard S, Vercauteren K, 1380  
 Verhoye L, Wychowski C, Leroux-Roels G, Palmer KE, 1381  
 Dubuisson J. Griffithsin has antiviral activity against 1382  
 hepatitis C virus. *Antimicrob Agents Chemother* 2011; 1383  
 55:5159–5167. 1384
29. Helle F, Wychowski C, Vu-Dac N, Gustafson KR, 1385  
 Voisset C, Dubuisson J. Cyanovirin-N inhibits hepatitis C 1386  
 virus entry by binding to envelope protein glycans. *J Biol* 1387  
*Chem* 2006;281:25177–25183. 1388
30. Hoque MM, Suzuki K, Tsunoda M, Jiang J, Zhang F, 1389  
 Takahashi A, Ohbayashi N, Zhang X, Tanaka H, 1390  
 Omura S, Takénaka A. Structural insights into the spe- 1391  
 cific anti-HIV property of actinohivin: structure of its 1392  
 complex with the  $\alpha(1-2)$ mannobiose moiety of gp120. 1393  
*Acta Crystallogr D Biol Crystallogr* 2012;68:1671–1679. 1394
31. Freedman H, Logan MR, Hockman D, Koehler Leman J, 1395  
 Law JLM, Houghton M. Computational prediction of the 1396  
 heterodimeric and higher-order structure of gpE1/gpE2 1397  
 envelope glycoproteins encoded by hepatitis C virus. 1398  
*J Virol* 2017;91:e02309–e02316. 1399
32. Cholankeril G, Ahmed A. Alcoholic liver disease replaces 1400  
 hepatitis C virus infection as the leading indication for 1401  
 liver transplantation in the United States. *Clin Gastro-* 1402  
*enterol Hepatol* 2018;16:1356–1358. 1403
33. Wali M, Harrison R, Gow P, Mutimer D. Advancing donor 1404  
 liver age and rapid fibrosis progression following trans- 1405  
 plantation for hepatitis C. *Gut* 2002;51:248–252. 1406
34. Colpitts CC, Chung RT, Baumert TF. Entry inhibitors: a 1407  
 perspective for prevention of hepatitis C virus infection in 1408  
 organ transplantation. *ACS Infect Dis* 2017;3:620–623. 1409
35. Baumert TF, Jühling F, Ono A, Hoshida Y. Hepatitis C- 1410  
 related hepatocellular carcinoma in the era of new gen- 1411  
 eration antivirals. *BMC Med* 2017;15:52. 1412
36. Colpitts C, Baumert T. Addressing the challenges of 1413  
 hepatitis C virus resistance and treatment failure. Multi- 1414  
 disciplinary Digital Publishing Institute, 2016. 1415

- 1415 37. Colpitts CC, Tsai PL, Zeisel MB. Hepatitis C virus entry: 1474  
 1416 an intriguingly complex and highly regulated process. *Int* 1475  
 1417 *J Mol Sci* 2020;21:2091. 1476
- 1418 38. Terrault N, Shrestha R, Satapathy SK, O'Leary JG, 1477  
 1419 Campsen J, Rosenau J, Spivey J, Teperman LW, 1478  
 1420 Therapondos G, Verna EC, Vierling JM, Schiano TD, 1479  
 1421 Sher L, Khallafi H, Victor D, Bhamidimarri KR, 1480  
 1422 Gordon FD, Hanish S, Kulik LM, Lake-Bakaar G, Maluf D, 1481  
 1423 Porayko M, Bramer SL, Osgood G, Chavan S, Daelken N. 1482  
 1424 LP17: Novel approach for the prevention of recurrent 1483  
 1425 hepatitis C in liver transplant recipients: preliminary re- 1484  
 1426 sults from ongoing phase III trial with civacir. *J Hepatol* 1485  
 1427 2015;62:S271–S272. 1486
- 1428 39. Smith HL, Chung RT, Mantry P, Chapman W, Curry MP, 1487  
 1429 Schiano TD, Boucher E, Cheslock P, Wang Y, 1488  
 1430 Molrine DC. Prevention of allograft HCV recurrence 1489  
 1431 with peri-transplant human monoclonal antibody MBL- 1490  
 1432 HCV1 combined with a single oral direct-acting anti- 1491  
 1433 vidual: a proof-of-concept study. *J Viral Hepat* 2017; 1492  
 1434 24:197–206. 1493
- 1435 40. Helle F, Goffard A, Morel V, Duverlie G, McKeating J, 1494  
 1436 Keck Z-Y, Fong S, Penin F, Dubuisson J, Voisset C. The 1495  
 1437 neutralizing activity of anti-hepatitis C virus antibodies is 1496  
 1438 modulated by specific glycans on the E2 envelope pro- 1497  
 1439 tein. *J Virol* 2007;81:8101–8111. 1498
- 1440 41. Pantua H, Diao J, Uitsch M, Hazen M, Mathieu M, 1499  
 1441 McCutcheon K, Takeda K, Date S, Cheung TK, Phung Q. 1500  
 1442 Glycan shifting on hepatitis C virus (HCV) E2 1501  
 1443 glycoprotein is a mechanism for escape from broadly 1502  
 1444 neutralizing antibodies. *J Mol Biol* 2013; 1503  
 1445 425:1899–1914. 1504
- 1446 42. Balzarini J. Targeting the glycans of glycoproteins: a 1505  
 1447 novel paradigm for antiviral therapy. *Nat Rev Microbiol* 1506  
 1448 2007;5:583–597. 1507
- 1449 43. Peters L, Klein MB. Epidemiology of hepatitis C virus in 1508  
 1450 HIV-infected patients. *Curr Opin HIV AIDS* 2015; 1509  
 1451 10:297–302. 1510
- 1452 44. Schranz AJ, Barrett J, Hurt CB, Malvestutto C, Miller WC. 1511  
 1453 Challenges facing a rural opioid epidemic: treatment and 1512  
 1454 prevention of HIV and hepatitis C. *Curr HIV/AIDS Rep* 1513  
 1455 2018;15:245–254. 1514
- 1456 45. Ruck JM, Segev DL. Expanding deceased donor kidney 1515  
 1457 transplantation: medical risk, infectious risk, hepatitis C 1516  
 1458 virus, and HIV. *Curr Opin Nephrol Hypertens* 2018; 1517  
 1459 27:445–453. 1518
- 1460 46. Bodzin AS, Baker TB. Liver transplantation today: where 1519  
 1461 we are now and where we are going. *Liver Transpl* 2018; 1520  
 1462 24:1470–1475. 1521
- 1463 47. Nakabayashi H, Taketa K, Miyano K, Yamane T, Sato J. 1522  
 1464 Growth of human hepatoma cell lines with differentiated 1523  
 1465 functions in chemically defined medium. *Cancer Res* 1524  
 1466 1982;42:3858–3863. 1525
- 1467 48. Wakita T, Pietschmann T, Kato T, Date T, Miyamoto M, 1526  
 1468 Zhao Z, Murthy K, Habermann A, Kräusslich H-G, 1527  
 1469 Mizokami M. Production of infectious hepatitis C virus in 1528  
 1470 tissue culture from a cloned viral genome. *Nat Med* 2005; 1529  
 1471 11:791. 1530
- 1472 49. Goueslain L, Alsaleh K, Horellou P, Roingeard P, 1531  
 1473 Descamps V, Duverlie G, Ciczora Y, Wychowski C, 1532  
 Dubuisson J, Rouillé Y. Identification of GBF1 as a 1533  
 cellular factor required for hepatitis C virus RNA repli- 1474  
 cation. *J Virol* 2010;84:773–787. 1475
50. Maurin G, Fresquet J, Granio O, Wychowski C, Cosset F- 1476  
 L, Lavillette D. Identification of interactions in the E1E2 1477  
 heterodimer of hepatitis C virus important for cell entry. 1478  
*J Biol Chem* 2011;286:23865–23876. 1479
51. Scheel TK, Gottwein JM, Jensen TB, Prentoe JC, 1480  
 Hoegh AM, Alter HJ, Eugen-Olsen J, Bukh J. Develop- 1481  
 ment of JFH1-based cell culture systems for hepatitis C 1482  
 virus genotype 4a and evidence for cross-genotype 1483  
 neutralization. *Proc Natl Acad Sci U S A* 2008; 1484  
 105:997–1002. 1485
52. Jensen TB, Gottwein JM, Scheel TK, Hoegh AM, Eugen- 1486  
 Olsen J, Bukh J. Highly efficient JFH1-based cell-culture 1487  
 system for hepatitis C virus genotype 5a: failure of ho- 1488  
 mologous neutralizing-antibody treatment to control 1489  
 infection. *J Infect Dis* 2008;198:1756–1765. 1490
53. Gottwein JM, Scheel TK, Jensen TB, Lademann JB, 1491  
 Prentoe JC, Knudsen ML, Hoegh AM, Bukh J. Develop- 1492  
 ment and characterization of hepatitis C virus geno- 1493  
 type 1–7 cell culture systems: role of CD81 and 1494  
 scavenger receptor class B type I and effect of antiviral 1495  
 drugs. *Hepatology* 2009;49:364–377. 1496
54. De Beeck AO, Voisset C, Bartosch B, Ciczora Y, 1497  
 Cocquerel L, Keck Z, Fong S, Cosset F-L, Dubuisson J. 1498  
 Characterization of functional hepatitis C virus envelope 1499  
 glycoproteins. *J Virol* 2004;78:2994–3002. 1500
55. Dubuisson J, Hsu HH, Cheung RC, Greenberg HB, 1501  
 Russell DG, Rice CM. Formation and intracellular local- 1502  
 ization of hepatitis C virus envelope glycoprotein com- 1503  
 plexes expressed by recombinant vaccinia and Sindbis 1504  
 viruses. *J Virol* 1994;68:6147–6160. 1505
56. Zhang Y, Huo M, Zhou J, Xie S. PKSolver: An add-in 1506  
 program for pharmacokinetic and pharmacodynamic 1507  
 data analysis in Microsoft Excel. *Comput Methods Pro- 1508  
 grams Biomed* 2010;99:306–314. 1509
57. Ji C, Liu Y, Pamulapati C, Bohini S, Fertig G, 1510  
 Schraeml M, Rubas W, Brandt M, Ries S, Ma H, 1511  
 Klumpp K. Prevention of hepatitis C virus infection 1512  
 and spread in human liver chimeric mice by an anti-CD81 1513  
 monoclonal antibody. *Hepatology* 2015;61:1136–1144. 1514
58. Takeuchi T, Katsume A, Tanaka T, Abe A, Inoue K, 1515  
 Tsukiyama-Kohara K, Kawaguchi R, Tanaka S, 1516  
 Kohara M. Real-time detection system for quantification 1517  
 of hepatitis C virus genome. *Gastroenterology* 1999; 1518  
 116:636–642. 1519

Received May 20, 2020. Accepted August 25, 2020.

#### Correspondence

Address correspondence to: Nobuyuki Matoba, Department of Pharmacology and Toxicology, University of Louisville School of Medicine, 505 S Hancock Street, Room 615, Louisville, Kentucky 40202. e-mail: [n.matoba@louisville.edu](mailto:n.matoba@louisville.edu); fax: (xxx) xxx-xxxx.

#### Acknowledgments

CRedit Authorship Contributions: Matthew Dent (Data curation: Equal; Formal analysis: Lead; Investigation: Equal; Validation: Supporting; Writing – original draft: Lead); Krystal Hamorsky (Formal analysis: Supporting; Writing – review & editing: Supporting); Thibaut Vaussele (Data curation: Equal; Formal analysis: Equal; Investigation: Supporting; Writing – review & editing: Supporting); Jean Dubuisson (Formal analysis: Supporting; Funding acquisition: Supporting; Investigation: Supporting; Methodology: Supporting; Supervision: Supporting; Validation: Equal; Writing – review & editing: Supporting).

1533	Supporting); Yoshinari Miyata (Data curation: Supporting; Formal analysis: Supporting; Investigation: Supporting; Methodology: Supporting; Project administration: Supporting; Validation: Equal; Writing – review & editing: Supporting); Yoshio Morikawa (Investigation: Supporting; Project administration: Supporting; Supervision: Supporting; Validation: Supporting; Writing – review & editing: Supporting); Nobuyuki Matoba, PhD (Conceptualization: Lead; Data curation: Equal; Formal analysis: Supporting; Funding acquisition: Lead; Investigation: Lead; Methodology: Lead; Project administration: Lead; Supervision: Lead; Validation: Equal; Writing – original draft: Supporting; Writing – review & editing: Lead).	immunofluorescence analyses were performed with the help of the imaging core facility of the Bioluminescence Center Lille Nord-de-France.	1592
1534			1593
1535			1594
1536		<b>Conflicts of interest</b>	1595
1537		This author discloses the following: Nobuyuki Matoba is an inventor on a patent concerning the composition and utility of Avaren-Fc (US patent number 8802822). The remaining authors disclose no conflicts.	1596
1538			1597
1539		<b>Funding</b>	1598
1540	The authors thank Adeline Danneels, Lucie Fénéant, Czeslaw Wychowski, Lauren Moore, and Jessica Jurkiewicz for their experimental help. The authors also are grateful to R. Bartenschlager, J. Bukh, F.L. Cosset, M. Harris, and T. Wakita for providing essential reagents. The	This work was supported by the University of Louisville ExCITE program, which was funded by US National Institutes of Health (U01 HL127518) and the Leona M. and Harry B. Helmsley Charitable Trust. Avaren-Fc <sup>lec-</sup> was created from work supported by a National Institutes of Health grant (R33 AI088585).	1599
1541			1600
1542			1601
1543			1602
1544			1603
1545			1604
1546			1605
1547			1606
1548			1607
1549			1608
1550			1609
1551			1610
1552			1611
1553			1612
1554			1613
1555			1614
1556			1615
1557			1616
1558			1617
1559			1618
1560			1619
1561			1620
1562			1621
1563			1622
1564			1623
1565			1624
1566			1625
1567			1626
1568			1627
1569			1628
1570			1629
1571			1630
1572			1631
1573			1632
1574			1633
1575			1634
1576			1635
1577			1636
1578			1637
1579			1638
1580			1639
1581			1640
1582			1641
1583			1642
1584			1643
1585			1644
1586			1645
1587			1646
1588			1647
1589			1648
1590			1649
1591			1650